npj | vaccines

Article

Published in partnership with the Sealy Institute for Vaccine Sciences

https://doi.org/10.1038/s41541-025-01356-x

Multi-antigen DNA vaccine targeting non-structural proteins confers robust T Cell-mediated protection against Zika virus

Ryan Santos[1,6], Zelalem A. Mekonnen[1,6], Arthur Eng Lip Yeow[1], Dawn M. Whelan[1], Zahraa Al-Delfi[1], Nicholas S. Eyre[2], Michael R. Beard[3], Dan H. Barouch[4], David H. O'Connor[5], Makutiro G. Masavuli[1,7] & Branka Grubor-Bauk[1,7] ✉

Zika virus (ZIKV) vaccine development has been hindered by the risk of antibody-dependent enhancement (ADE), particularly in dengue-endemic regions, where sub-neutralizing antibodies can exacerbate disease severity. T cell-based vaccines targeting non-structural (NS) antigens represent a safer alternative that bypasses this risk. Using immunocompetent BALB/c mice, we performed high-resolution in vivo mapping of ZIKV specific $CD8^+$ and $CD4^+$ T cell responses following $ZIKV_{PRVABC59}$ infection, identifying high avidity, polyfunctional memory T cells targeting conserved NS1, NS3 and NS4 proteins. Guided by these data, we developed DNA vaccines encoding full-length NS3 and NS4 and evaluated their efficacy against ZIKV infection alone or combined with a validated construct encoding secreted NS1 (p-tpaNS1). NS3 and NS4 vaccination elicited robust cytotoxic and IFN-γ producing T cell responses, while co-administration with p-tpaNS1 significantly reduced peak serum viremia achieving earlier and stronger viral control. Although NS1 alone conferred strong protection, the multi-antigen formulation demonstrated additive benefits. This T cell-based vaccine approach, targeting conserved NS proteins, offers a scalable, thermostable platform with potential for safe deployment in childbearing women and resource-limited regions. Given NS protein conservation and cross-reactivity across flaviviruses, it also provides a promising foundation for next-generation pan-flavivirus vaccine development, although this remains to be directly tested.

Zika virus (ZIKV) is a re-emerging mosquito-borne flavivirus closely related to dengue (DENV), yellow fever (YFV), Japanese encephalitis (JEV), tick-borne encephalitis (TBEV), and West Nile viruses (WNV). Maintained in a sylvatic cycle between non-human primates and mosquitoes, ZIKV periodically spills into human populations[1], with persistent endemic transmission in parts of Asia and the Americas since the 2015–16 epidemic[2,3]. While ZIKV is primarily transmitted by *Aedes* mosquitoes, sexual, blood-borne, and vertical transmission routes have been documented[4–6]. Vertical transmission poses particular risks during early pregnancy, with increased rates of fetal loss, microcephaly, and developmental abnormalities[7–10]. Clinically, ZIKV is associated with neuro-inflammatory syndromes across age groups. In adults, the virus can trigger Guillain–Barré syndrome, resulting in peripheral nerve damage, paralysis, and long-term disability[11–13]. In neonates, vertical transmission can lead to congenital Zika syndrome, characterized by microcephaly and lifelong neurodevelopmental impairments[14–17].

Despite substantial efforts, no licensed vaccine or antiviral therapy is available. The need for a safe, broadly protective vaccine remains urgent, particularly for pregnant women and individuals in endemic regions. Vaccine strategies to date have primarily focused on the viral envelope (E) protein to induce neutralizing antibodies[18,19]. However, E-targeted approaches raise safety concerns due to antibody-dependent

[1]Viral Immunology Group, Adelaide Medical School, The University of Adelaide and Basil Hetzel Institute for Translational Health Research, Adelaide, SA, Australia. [2]Molecular Virology Group, College of Medicine and Public Health, Flinders University, Adelaide, SA, Australia. [3]Research Centre for Infectious Diseases, School of Biological Sciences, University of Adelaide, Adelaide, SA, Australia. [4]Centre for Virology and Vaccine Research, Beth Israel Deaconess Medical Centre, Harvard Medical School, Boston, MA, USA. [5]Department of Pathology and Laboratory Medicine, University of Wisconsin–Madison, Madison, WI, USA. [6]These authors contributed equally: Ryan Santos, Zelalem A. Mekonnen. [7]These authors jointly supervised this work: Makutiro G. Masavuli, Branka Grubor-Bauk. ✉e-mail: branka.grubor@adelaide.edu.au

enhancement (ADE) of infection, a phenomenon where cross-reactive, sub-neutralizing antibodies facilitate Fcγ receptor-mediated viral entry and exacerbate disease[20]. ADE has been well documented in DENV and shown to occur bidirectionally between DENV and ZIKV in mice[21–23], macaques[24,25], and epidemiological cohorts[21–23,25–27]. These findings underscore the need for alternative vaccine strategies that avoid or minimize ADE risk.

In addition to these immunological concerns, clinical development of ZIKV vaccines has also been constrained by the decline in ZIKV incidence since the 2015–16 epidemic[28]. The low number of clinically apparent cases has reduced the feasibility of efficacy trials and limited investment in large-scale development[29]. Thus, while the primary barrier to clinical progress has been epidemiological and logistical, the potential for vaccine-induced ADE remains a key design consideration for safe deployment, particularly in dengue-endemic regions.

Non-structural (NS) proteins (NS1, NS3, NS4B, and NS5) are critical for viral replication and immune evasion but are not displayed on mature virions and therefore do not induce ADE-associated antibodies. These antigens elicit robust $CD4^+$ and $CD8^+$ T cell responses that are critical for virus clearance and immune memory[30–35]. Human and mouse studies have shown that T cells targeting conserved NS3, NS4B, and NS5 can mediate protection against ZIKV and DENV[36–38], with cross-reactive responses observed in individuals with prior exposure to JEV or DENV[36,39–43]. While our study focuses specifically on ZIKV, these prior findings suggest that NS proteins may hold promise as broadly protective targets for future pan-flavivirus vaccine development.

We previously demonstrated that a DNA vaccine encoding secreted NS1 (p-tpaNS1) protects against ZIKV challenge via T cell immunity, independent of neutralizing antibodies[44]. To expand immunological breadth, we next targeted additional conserved NS antigens, NS3 and NS4, aiming to enhance $CD8^+$ T cell breadth, durability, and cross-reactivity. Multi-antigen vaccine formulation has shown superior immunogenicity and protection for other pathogens[45–48], improving T cell breadth, functional quality, and long-term immunity. Applying this approach to ZIKV offers a rational strategy to induce broad, protective T cell responses while avoiding structural antigens associated with ADE.

A precise understanding of immunodominant ZIKV NS epitopes in an immunocompetent host is essential for applying NS-directed T cell immunity into an effective vaccine design. Previous T cell epitope-mapping studies have relied on interferon-deficient or HLA transgenic mice, models which only partially recapitulate native responses and can skew antigen dominance patterns[31,41,49]. To define immunodominant epitopes in an intact immune milieu, we mapped $CD4^+$ and $CD8^+$ T cell responses in wild-type BALB/c mice following ZIKV infection. To address this limitation, we performed high-resolution in vivo epitope mapping in wild-type BALB/c mice, capturing both the effector-contraction phase and the early memory phase. For each epitope, we quantified functional avidity and used multi-parameter intracellular cytokine staining to delineate polyfunctional $CD4^+$ and $CD8^+$ T cell profiles. This approach allowed direct assessment of the durability and functional quality of NS-specific cellular immunity.

Informed by the epitope mapping data, we generated plasmid DNA constructs encoding full-length NS3 and NS4 and examined them individually and in combination with a previously validated DNA vaccine encoding a secreted form of NS1 (p-tpaNS1)[44]. A multi-antigen formulation was selected to maximize the breadth and durability of cellular immunity while avoiding structural proteins implicated in ADE. Evidence from human cohort studies further supports this strategy: ZIKV NS3 and NS4B have emerged as dominant $CD8^+$ T cell targets across diverse HLA backgrounds in populations from both the Americas and Asia[50,51].

By engineering a DNA-based multi-antigen vaccine that avoids structural proteins, our platform circumvents ADE and instead prioritizes cellular immunity, a paradigm shift from most ZIKV vaccines currently in clinical development, which focus on the ZIKV E protein and face limitations in dengue-exposed populations[52–55].

Collectively, our study highlights a rational, multi-antigen DNA vaccine strategy that targets conserved NS proteins to elicit broad T cell immunity while avoiding ADE. This platform offers a promising route toward safe and effective vaccination against ZIKV and other flaviviruses.

Results

ZIKV infection induces broad effector T cell responses that contract into memory pools focused on NS1, NS3 and NS4

To delineate the kinetics of ZIKV-specific T-cell immunity, BALB/c mice were intravenously (*i.v*) infected with 200 plaque forming units (PFU) of $ZIKV_{PRVABC59}$[44,56]. Cytotoxic $CD8^+$ T lymphocyte (CTL) activity and $CD4^+$ T helper responses (Th) were assessed at days 7 (peak effector), 14 (contraction), and 35 (early memory) post-infection using the fluorescent target array (FTA) assay (Fig. 1A). These timepoints were selected based on established ZIKV T cell response dynamics in mouse models[57–59]. Gating strategy and peptide pools are shown in Supplementary Fig. 1.

At day 7, robust $CD8^+$ CTL activity was observed across peptide pools (P1-PX) spanning NS1–NS5 and Env (Fig. 1B), with significant responses to NS1-P2, NS2-P2, NS3-P1/2/3, NS4-P1/2, NS5-P1/2/3/5, and Env-P1/2/5/6 (Fig. 1C), indicating a broad and highly cytolytic effector-phase response. $CD4^+$ Th responses, measured by CD69 upregulation on $B220^+$ target cells, showed a similar breadth, with strong responses to peptide pools from NS1, NS2, NS3, NS4, NS5, and Env. Notably, NS1-P2, NS3-P5, and NS5-P2 elicited the highest Th activation at this phase. Peptide pools that did not elicit significant T cell responses are shown in Supplementary Fig. 1. By day 14, both CTL and Th responses showed marked contraction, consistent with the resolution of acute infection.

Antigens that prime robust and durable $CD8^+$ and $CD4^+$ T cell responses are more likely to confer protection, making them strong candidates for vaccine inclusion[60–62]. Therefore, Day 35 post-infection was chosen to evaluate the establishment of early immunological memory. At this stage, $CD8^+$ CTL activity was largely focused on NS1-P4, NS3-P3, NS4-P1/2, and Env-P1, indicating selective retention of memory CTLs (Fig. 1B), while $CD4^+$ responses were limited to NS1-P3 (Fig. 1C), indicating selective persistence of memory T cells.

Collectively, these data show that ZIKV infection elicits a broad, multi-antigenic effector T cell response that undergoes temporal contraction, yielding memory populations focused on NS1, NS3, and NS4. These NS proteins represent promising targets for T cell-based vaccine strategies due to their ability to support both effector and durable immunity.

High-resolution mapping identifies immunodominant ZIKV epitopes focused in NS1, NS3, NS4, and Env

To define specific T cell epitopes driving memory responses, we performed high-resolution FTA analysis at day 35 post-infection using 246 overlapping peptides spanning immunodominant pools from NS1, NS3, NS4, and Env (Fig. 2A). Peptide pool controls confirmed assay performance and induced strong positive responses (Fig. 2B, C; Gating strategy in Supplementary Fig. 2).

For $CD8^+$ T cells, discrete epitopes were identified in all three NS proteins. Within NS1-P4, three overlapping peptides ($NS1_{(259-273)}$, $NS1_{(262-276)}$, $NS1_{(265-279)}$), each containing the conserved core motif PWHSEELEI, emerged as dominant CTL targets. Additional $CD8^+$ T cell epitopes included $NS3_{298–312}$ (NS3-P3), $NS4_{183–200}$ (NS4-P1), and two overlapping NS4-P2 peptides ($NS4_{225–242}$ and $NS4_{232–249}$), sharing the motif "KGMPFYAWDFG". One epitope from Env ($Env_{58–72}$) also showed significant CTL activity (Fig. 2B).

For $CD4^+$ T helper responses, two overlapping peptides within NS1-P3 ($NS1_{202–216}$ and $NS1_{205–219}$) containing the core motif "NDTWRLKRAHLI" induced significant CD69 upregulation on $B220^+$ target cells, indicating strong Th activation (Fig. 2C). No additional class-II epitopes met significance at day 35. A summary of all immunodominant peptides is provided in Table 1.

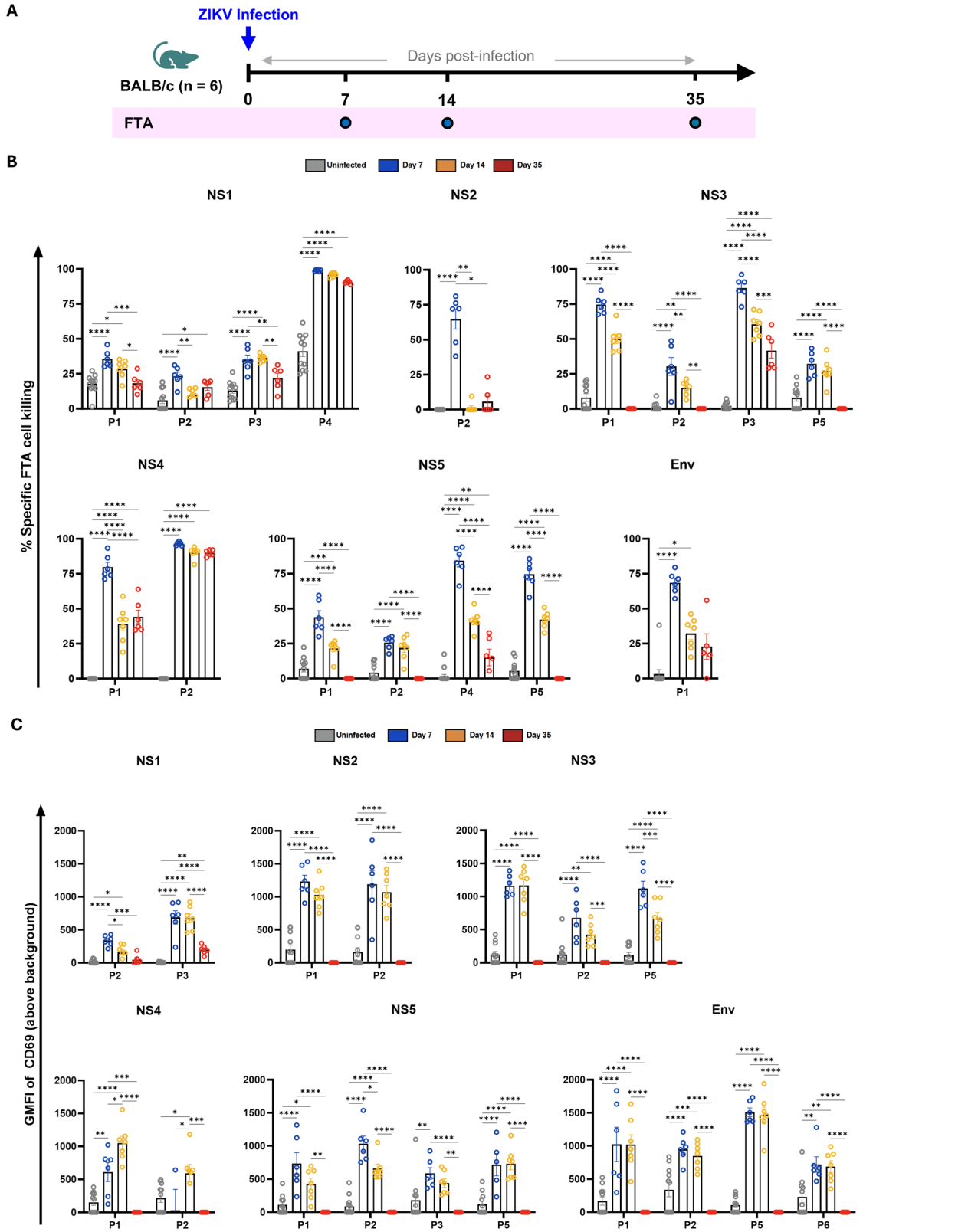

Fig. 1 | Temporal dynamics of ZIKV-specific T cell responses following infection in BALB/c mice. A Experimental timeline. Female BALB/c mice ($n = 5–7$/ group) were infected intravenously with 200 PFU of $ZIKV_{PRVABC59}$. On days 7 (effector phase), 14 (contraction phase), or 35 (early memory phase) post-infection, mice were intravenously injected with autologous splenocytes from naïve mice, which were pulsed with ZIKV peptide pools (PX) spanning NS1–NS5 and Env proteins and labeled with unique combinations of cell tracking dyes (CellTrace Violet CTV, Carboxyfluorescein Succinimidyl Ester CFSE, Cell Proliferation Dye eFluor 670 - CPD). **B** $CD8^+$ T cell cytotoxicity against peptide-pulsed targets was quantified using the fluorescent target array (FTA) assay. Graph shows mean ± SEM percentage specific killing for each peptide pool at the indicated timepoints. **C** $CD4^+$ T helper responses were assessed by measuring CD69 expression (geometric mean fluorescence intensity GMFI) on $B220^+$ peptide-pulsed target cells. Data represent mean ± SEM across timepoints. Low-responding pools are shown in Supplementary Fig. 1. Statistical comparisons were performed using two-way ANOVA with Tukey's multiple comparisons test. *$P < 0.05$, **$P < 0.01$, ***$P < 0.001$, ****$P < 0.0001$.

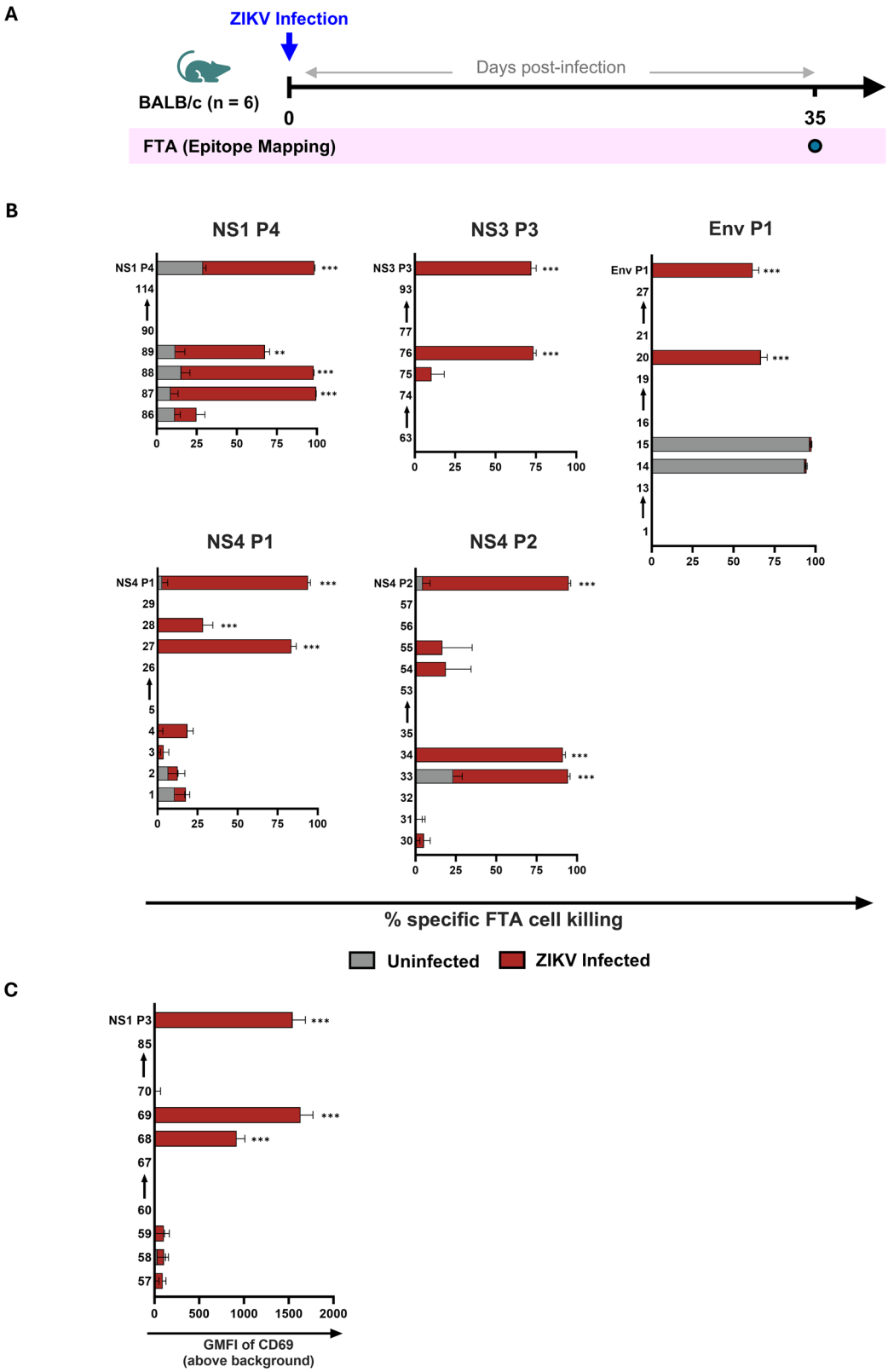

Fig. 2 | In vivo identification of immunodominant T cell epitopes in ZIKV-infected mice. A Schematic of epitope mapping experiment. Female BALB/c mice ($n = 5$/group) were infected i.v. with 200PFU of $ZIKV_{PRVABC59}$. On day 35 post-infection, mice were injected i.v. autologous splenocytes labeled with unique combinations of cell-tracking dyes (CTV, CFSE, CPD) and pulsed with 246 overlapping peptides spanning NS1, NS3, NS4, and Env regions previously identified as immunodominant pools. **B** $CD8^+$ T cell cytotoxic responses were quantified using FTA. Mean ± SEM percentage specific killing of individual peptide-pulsed targets is shown, compared to uninfected controls. **C** $CD4^+$ T cell responses were measured by CD69 upregulation on $B220^+$ peptide-pulsed targets. Data are presented as GMFI ± SEM for each peptide cluster. Statistical comparisons were performed using two-way ANOVA with Tukey's multiple comparisons test.
$^{**}P < 0.01$; $^{***}P < 0.001$.

Table 1 | Immunodominant epitopes detected at day 35 post-infection

Protein	Peptide pool	Peptide number	Sequence position (a.a.)	Peptide	Peptide length	CTL/Th T cell targets
NS1	P3	68	202–216	SEK**NDTWRLKRAHLI**	15	Th
		69	205–219	**NDTWRLKRAHLI**EMK	15	
	P4	87	259–273	RTQMKG**PWHSEELEI**	15	CTL
		88	262–276	MKG**PWHSEELEI**RFE	15	
		89	265–279	**PWHSEELEI**RFEECP	15	
NS3	P3	76	298–312	RGYISTRVEMGEAAA	15	
NS4	P1	27	183–200	DLRPASAWAIYAALTTFI	18	
	P2	33	225–242	GVLFGMG**KGMPFYAWDFG**	18	
		34	232–249	**KGMPFYAWDFG**VPLLMIG	18	
Env	P1	20	58–72	SYCYEASISDMASDS	15	

Bolded amino acid residues represent the overlapping sequence shared between consecutive peptides.

These data refine the immunodominant T cell repertoire elicited by ZIKV infection and pinpoint discrete NS1, NS3, and NS4 regions as high-priority candidates for inclusion in T cell–based vaccine platforms.

ZIKV infection induces high avidity, polyfunctional CD8$^+$ T cell responses targeting NS1, NS3, and NS4

To assess the functional quality of ZIKV-specific T cells, we evaluated antigen sensitivity (functional avidity) and cytokine polyfunctionality using in vivo FTA (Fig. 3A) and in *vitro* intracellular cytokine staining (ICS; Fig. 4A) during the effector and early memory phases. Immunodominant epitopes identified at day 35 post-infection were used as peptide stimuli.

To measure functional avidity, FTA target cells were pulsed with graded peptide concentrations (10–0.01 μg/mL). During the effector phase, NS4-derived epitopes $NS4_{183–200}$ and $NS4_{232–249}$ elicited CTL responses at concentrations as low as 0.1 μg/mL, while other epitopes required ≥1 μg/mL for significant killing (Fig. 3B). These high avidity responses persisted into the memory phase (day 35) except for $NS3_{298–312}$. For CD4$^+$ T helper responses, $NS1_{202–216}$ and $NS1_{205–219}$ upregulated CD69 on B220$^+$ targets at 1 μg/mL (Fig. 3C), indicating strong T helper cell activation. These findings demonstrate that ZIKV infection generates T cells with high antigen sensitivity, supporting their capacity for effective anti-viral function in vivo.

To assess functional breadth, we analyzed cytokine production in CD44^{high}CD62L$^-$ effector memory CD8$^+$ T cells (CD8$^+$$T_{EM}$) using ICS. Compared to mock-infected controls, ZIKV infection significantly increased the frequency of IFN-γ, TNF-α and IL-2 CD8$^+$ T_{EM} cells (Fig. 4B–E). NS4 P2 epitopes ($NS4_{225–242}$ and $NS4_{232–249}$) induced the highest responses across all cytokines measured, followed by NS1 P4 ($NS1_{259–273}$, $NS1_{262–276}$). Modest but detectable responses were observed for NS4 P1, $NS4_{183–200}$, NS3 P3 ($NS3_{298–312}$), and $Env_{58–72}$ (Fig. 4).

Polyfunctionality was highest in response to NS4 P2 epitopes, which generated dual IFN-γ$^+$/IL-2$^+$ (Fig. 4F) and IFN-γ$^+$/TNF-α$^+$ (Fig. 4G), as well as triple positive IFN-γ$^+$/TNF-α$^+$/IL-2$^+$ CD8$^+$$T_{EM}$ cells (Fig. 4H). IFN-γ responses were the most prominent overall, particularly in response to NS4 P2 and NS1 P4, consistent with strong effector activation (Fig. 4C). TNF-α was the most broadly induced cytokine across all epitopes, including from lower avidity epitopes (Fig. 4D). This pattern suggests that TNF-α may occur at lower activation thresholds, making it a comparatively sensitive marker of antigen recognition, especially among partially activated or lower avidity T-cells[63]. IL-2 production was restricted to high-responder epitopes, primarily NS4 P2, $NS4_{225–242}$, and $NS4_{232–249}$ (Fig. 4E), reflecting their potential to promote memory differentiation. These epitopes also generated the highest frequencies of triple cytokine-producing CD8$^+$$T_{EM}$ cells, widely considered correlates of robust, durable immunity[59,64].

Dual-functional responses were dominated by IFN-γ$^+$/TNF-α$^+$ producers, particularly in response to NS4 P2 and NS1 P4. IFN-γ$^+$/IL-2$^+$ cells, while less frequent, were enriched within high-quality responses, reinforcing the capacity of these epitopes to support memory development. In contrast, responses to NS3 and Env peptides were largely monofunctional and exhibited limited polyfunctionality, underscoring the superior immunogenic profile of NS4-derived antigens. Dual expression of IL-2 and TNF-α was also assessed, but no significant differences were observed across peptide stimulations, and thus, not further emphasized (Supplementary Fig. 3).

Together, these results show that ZIKV infection elicits high-avidity, polyfunctional T cells that persist into the memory phase. Epitopes derived from NS1, NS3, and particularly NS4 support the strongest functional signatures, reinforcing their value as targets in T cell-focused vaccine design. We next evaluated the immunogenicity and protective potential of DNA vaccines encoding NS3 and NS4, individually and in combination with p-tpaNS1.

NS3 and NS4 DNA vaccines elicit potent CD8$^+$ T cell responses

We generated two codon optimized DNA vaccines encoding full length ZIKV NS3 (pNS3) and NS4 (pNS4), each cloned into the pVAX1 backbone under the control of a CMV promoter (Fig. 5A). Antigen expression was validated by indirect immunofluorescence in transfected HEK293T cells (Supplementary Fig. 4). BALB/c mice ($n = 7$) received three intradermal doses of 50 μg DNA vaccine at 2-week intervals (Fig. 5B) and T cell responses were assessed 2 weeks after the final dose.

ELISpot analysis revealed strong IFN-γ responses in pNS3 vaccinated mice, with highest responses directed against peptide pools P1, P2, P3, and P5 (mean SFU±SEM = 1077, 270, 2158, and 252, respectively; Supplementary Fig. 5A). Cumulative analysis confirmed the robust immunogenicity of pNS3 vaccine (Fig. 5C). Similarly, pNS4 vaccination induced significant IFN-γ responses to both NS4 peptide pools, with a dominant response to pool 2 (NS4B domain; mean SFU±SEM 1009.29) compared to pool 1 (mean SFU ± SEM 238.21) (Supplementary Fig. 5B, E).

In vivo cytotoxicity assessed by FTA corroborated the ELISpot results. In pNS3-immunized mice, strong CD8$^+$ T cell-mediated killing was observed for NS3 pools P1, P2, and P3 with mean killing percentages of 70.97%, 49.73%, 82.23%, respectively. (Fig. 5D). CD4$^+$ T helper responses, measured by CD69 expression on B220$^+$ target cells, were detected in response to NS3 P1 and P5 (GMFI: 232.14, 271.94, Fig. 5D). For pNS4, FTA confirmed significant cytotoxic responses against both NS4 P1 and P2 (mean killing: 15.57%, 41.80%, respectively; Fig. 5F), while CD4$^+$ Th responses were minimal.

Together, these findings demonstrate that both pNS3 and pNS4 vaccines induce strong, antigen-specific CD8$^+$ T cell immunity, with NS3 showing broader T cell activation, including helper responses. These results support the integration of NS3 and NS4 into a multi-antigen DNA vaccine to enhance protective T cell responses against ZIKV.

A multi-antigen NS1/NS3/4 DNA vaccine confers superior protection against ZIKV challenge

Based on immunogenicity profiling, we next assessed the protective efficacy of a multi-antigen DNA vaccine strategy. To maximize T cell breadth while minimizing formulation complexity, we generated a polyprotein construct

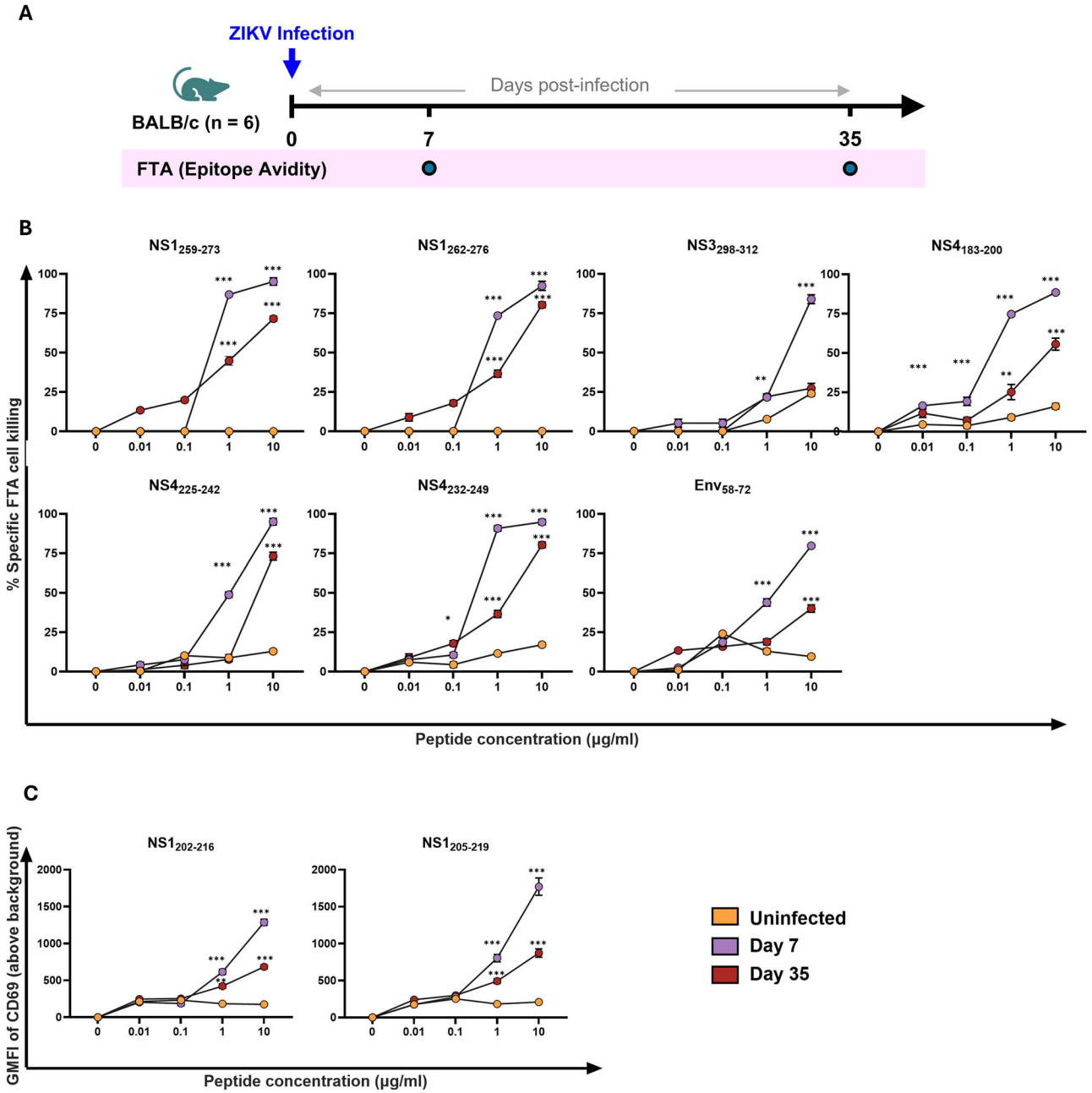

Fig. 3 | Functional avidity of ZIKV-specific CD8$^+$ and CD4$^+$ T cell responses. **A** Experimental timeline for peptide avidity analysis. Female BALB/c mice ($n = 5$/group) were infected with 200PFU of ZIKV$_{PRVABC59}$ or left uninfected (orange). On days 7 (purple) or 35-days (red) post-infection, mice were injected intravenously with naive splenocyte targets pulsed with serial dilutions (10–0.01 μg/mL) of immunodominant peptides identified in Fig. 2. **B** CD8$^+$ T cell cytotoxicity was quantified using the FTA assay. Data show mean ± SEM percentage specific killing at each peptide concentration for each target cluster (**C**) CD4$^+$ T cell activity was assessed by CD69 expression on B220$^+$ target cells pulsed with NS1$_{202\text{-}216}$ and NS1$_{205\text{-}219}$ peptides. Data represent GMFI ± SEM in ZIKV-infected and uninfected mice. Statistical comparisons using two-way ANOVA with Dunnett's post-hoc (vs. uninfected controls). * $P < 0.05$, ** $P < 0.01$, *** $P < 0.001$.

encoding NS3 and NS4 (pNS3/4) and co-administered it with our previously validated secreted NS1 vaccine (p-tpaNS1). This reduced the total formulation from three plasmids to two: p-tpaNS1 and pNS3/4 (Fig. 6A, B). NS1 was maintained as a standalone plasmid due to secretion-dependent immunogenicity, which was compromised when encoded in polyprotein configurations. Expression of NS1, NS3, and NS4 in each vaccine construct was validated by indirect immunofluorescence in transfected HEK293T (Supplementary Fig. 4).

BALB/c mice ($n = 10$ per group) received three ID doses of vaccine or pVAX (Fig. 6B): pVAX control (50 μg), p-tpaNS1 (50 μg), pNS3/4 (50 μg), or the cocktail (50 μg p-tpaNS1 + 50 μg pNS3/4). To ensure that co-administration of pNS3/4 did not impair NS1 immunogenicity, we measured anti-NS1IgG titers by ELISA after each dose. Antibody levels rose comparably in both p-tpaNS1 and cocktail groups, confirming that pNS3/4 co-delivery does not interfere with humoral responses to NS1 (Fig. 6C).

Three weeks after the final dose, mice were challenged intravenously with 200 PFU of ZIKV$_{PRVABC59}$. Serum viral loads (VL) were measured by RT-qPCR on days 1, 2, 3, and 7 post-challenge. All vaccine groups had significantly reduced viraemia on day 1 post-challenge, with the cocktail group showing the greatest VL reduction (mean ± SEM copies/ml p-tpaNS1: 3.6×10^4; pNS3/4: 1.34×10^5; cocktail: 9.3×10^3; Fig. 6D) when compared to pVAX control titers (1.1×10^6; ZIKV copies/mL; Fig. 6D). By day 2, the cocktail vaccine continued to outperform single components (mean ± SEM ZIKV copies/mL: p-tpaNS1: 9×10^3; pNS3/4: 1.94×10^4;

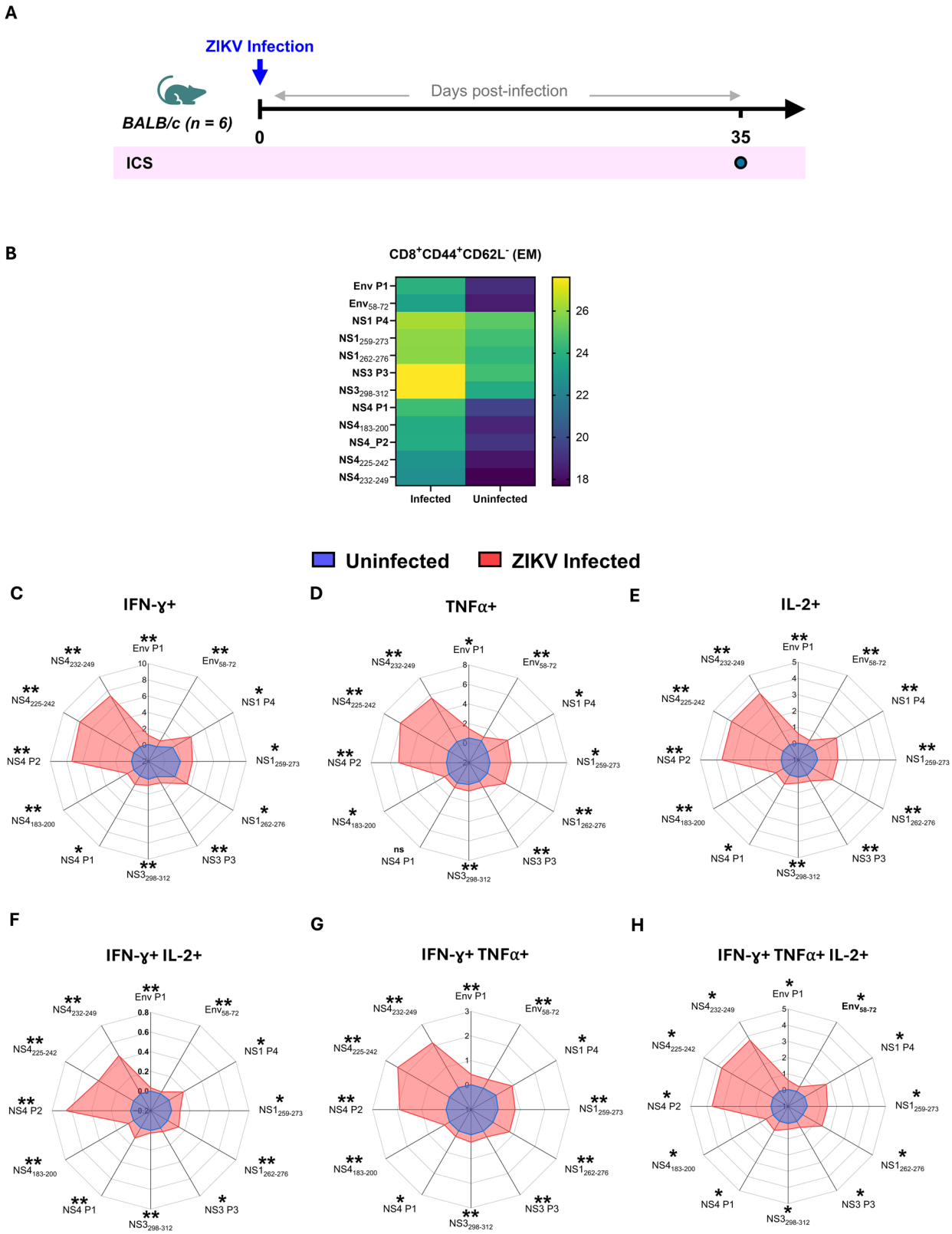

Fig. 4 | ZIKV infection elicits polyfunctional CD8⁺ effector memory T cell responses. A Experimental timeline for intracellular cytokine staining (ICS). Female BALB/c mice ($n = 5$/ group) were infected i.v. with 200PFU $ZIKV_{PRVABC59}$ or left uninfected. At day 35 post-infection, splenocytes were harvested and stimulated with mapped immunodominant ZIKV peptides for cytokine profiling. **B** Heatmap depicting the frequency of $CD44^{high}CD62L^{-}CD8^{+}$ effector memory (EM) T cells in ZIKV infected versus uninfected mice. Spider plots showing the frequency of (**C**) IFN-γ, (**D**) TNF-α and (**E**) IL-2 producing $CD8^{+}$ T_{EM} cells following peptide stimulation. Polyfunctionality analysis of $CD8^{+}$ T_{EM} cells showing dual cytokine expression (**F**) IFN-γ^{+} IL-2^{+}, (**G**) IFN-γ^{+} TNF-α^{+} and (**H**) IFN-γ^{+} TNF-α^{+} IL-2^{+}. Data are expressed as mean ± SEM. Statistical significance between groups was determined by Mann–Whitney U tests. To account for multiple testing, *p*-values were adjusted using the Benjamini–Hochberg false discovery rate (FDR) method $^{*}P < 0.05$, $^{**}P < 0.01$.

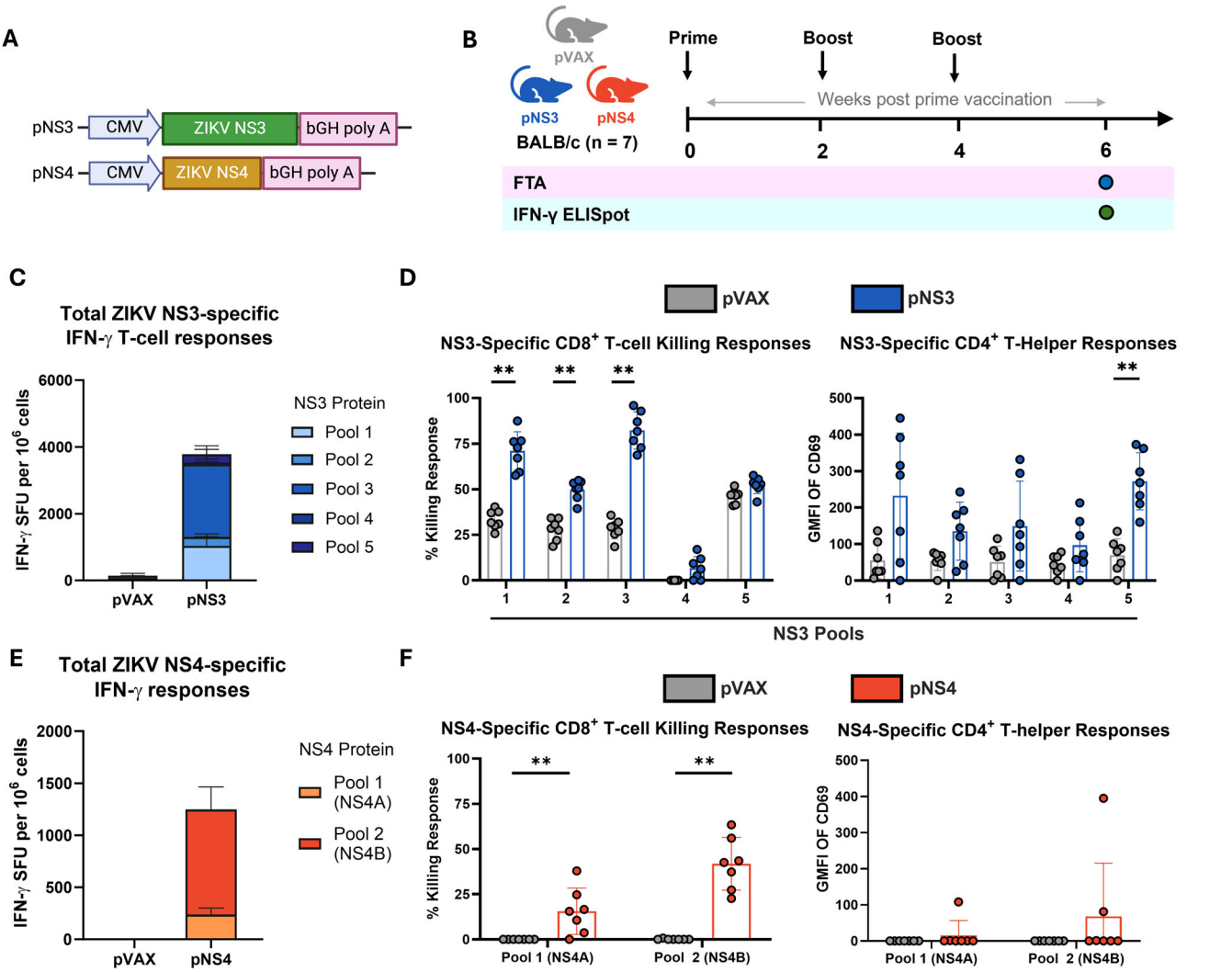

Fig. 5 | pNS3 and pNS4 DNA vaccines elicit robust CD8⁺ T cell responses against ZIKV non-structural proteins. A Schematic representation of the codon-optimized DNA vaccine constructs encoding full-length ZIKV NS3 (pNS3) and NS4 (pNS4), cloned into the pVAX1 vector under a CMV promoter. **B** Vaccination schedule. Female BALB/c mice (6–8 weeks old, $n = 7$/group) were immunized with 50 µg of pNS3, pNS4, or pVAX control, on days 0, 14, and 28. T cell responses were assessed 2 weeks after the final dose. **C** IFN-γ ELISpot quantification of total NS3-specific T cell responses following stimulation with five peptide pools spanning NS3. **D** Functional assessment of NS3-specific cytotoxic (CD8⁺) and helper (CD4⁺) T cell responses by in vivo fluorescent target array (FTA). Peptide pools P1–P5 (5 µg/mL) were used for stimulation. **E** IFN-γ ELISpot quantification of total NS4-specific T cell responses following stimulation with two peptide pools covering NS4A/B. **F** CTL and Th responses in pNS4-vaccinated mice as determined by in vivo FTA using NS4 peptide pools P1 and P2. Bars represent mean ± SEM; comparisons between groups were performed using Mann–Whitney U tests. To account for multiple testing, *p*-values were adjusted using the Benjamini–Hochberg false discovery rate (FDR) method. $^{**}P \leq 0.01$.

cocktail: 5.2×10^2) demonstrating significantly stronger viral control. On day 3, VL in the cocktail group declined further to 242 copies/mL, approaching the assay's limit of detection and indicating near-complete viral clearance. In contrast, pNS3/4 alone showed a reduction trend (1.6×10^3 copies/mL) that did not reach statistical significance. Control (pVAX) mice exhibited high viremia on days 1, 2, and 3 post-infection (mean ± SEM, ZIKV copies/mL: Day 1: 1.1×10^6; Day 2: 5.99×10^4; Day 3: 1.29×10^4; Fig. 6D). Taken together, these data show that pNS3/4 alone was less protective than p-tpaNS1, yet its inclusion in the cocktail provided earlier and more consistent viral clearance.

Discussion

The development of a safe and effective ZIKV vaccine remains an urgent global priority, complicated by the risk of ADE seen with flavivirus infections. Clinical data from heterologous DENV infections in Dengvaxia recipients[65,66] and longitudinal ZIKV and DENV cohort studies[26,67] have shown that sub-neutralizing ZIKV antibodies can exacerbate dengue disease, particularly DENV2. Maternal ZIKV antibodies were shown to enhance DENV disease in neonatal mice and vice versa, highlighting the dangers of relying on envelope antigens[21,26]. To eliminate this risk, we developed a T cell–based vaccine strategy targeting the conserved NS proteins (NS1, NS3, and NS4), thus avoiding structural antigens implicated in ADE.

Using an in vivo epitope mapping assay (FTA) in immunocompetent BALB/c mice, we identified robust, polyfunctional immunodominant CD8⁺ and CD4⁺ T-cell epitopes in ZIKV NS1, NS3, and NS4 after $ZIKV_{PRVABC59}$ infection. Unlike prior studies that relied on IFN-deficient models or ex vivo assays with limited resolution of in vivo epitope hierarchies[41,59,68,69], our work used a fully immunocompetent model and high-resolution, longitudinal epitope profiling to define immunodominance hierarchies and functional phenotypes. Dominant CD8⁺ T cell epitopes such as $NS4_{225–242}$ and $NS4_{232–249}$ elicited high-avidity responses with sustained memory and polyfunctionality (IFN-γ, TNF-α, and IL-2) that likely synergize to support antiviral activity,

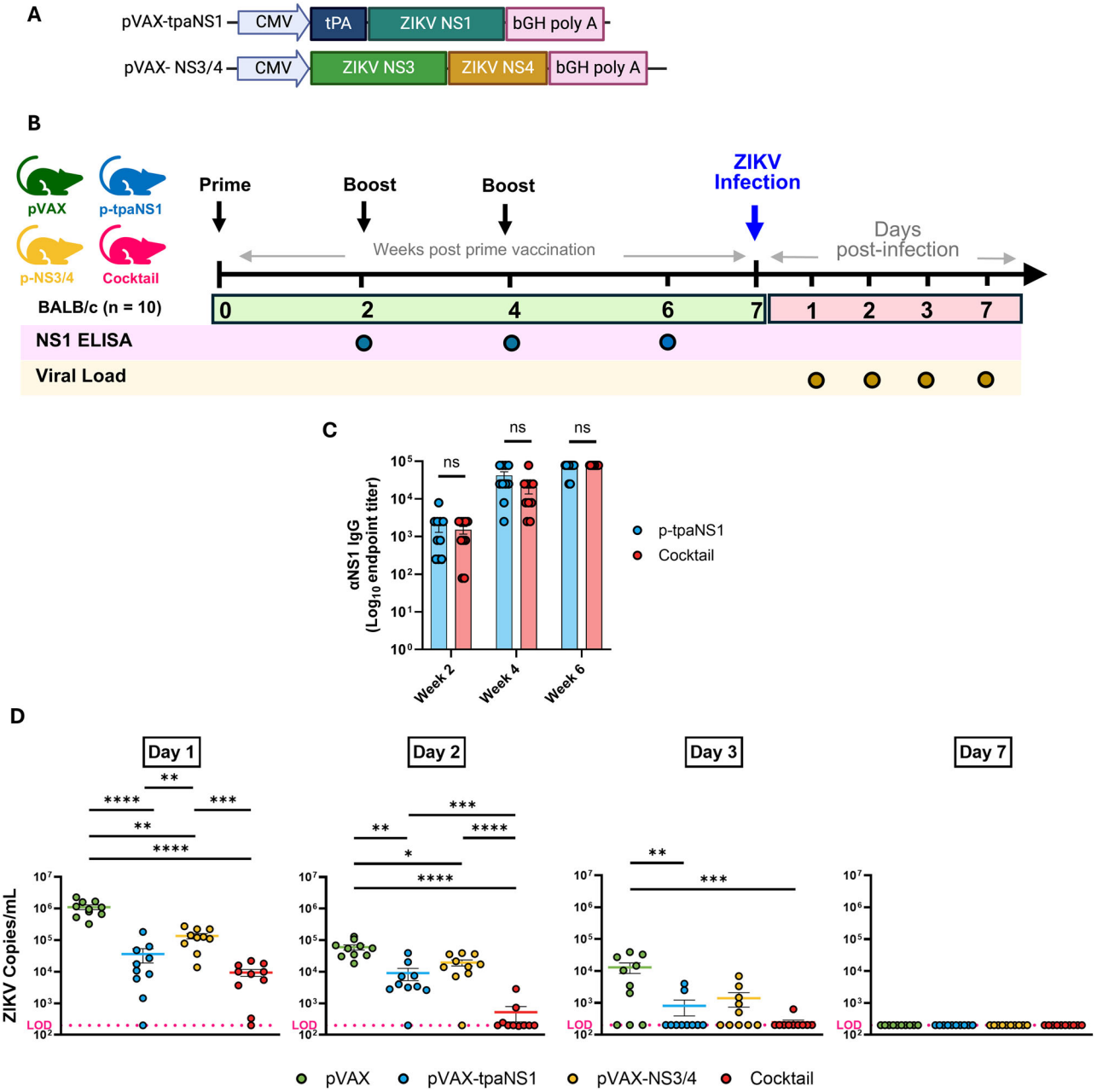

Fig. 6 | Multi-antigen DNA vaccine combining NS1, NS3, and NS4 confers superior protection against ZIKV challenge in BALB/c mice. A Schematic diagram of the two-plasmid vaccine formulation consisting of a secreted NS1 construct (p-tpaNS1) and a polyprotein construct encoding NS3 and NS4 (pNS3/4), both driven by CMV promoters in the pVAX1 backbone. **B** Vaccination and challenge timeline. Female BALB/c mice (6–8 weeks old, $n = 10$/group) received intradermal immunization with 50 µg of pVAX1 (control), p-tpaNS1, pNS3/4, or a combination of p-tpaNS1 + pNS3/4 (50 µg each). Two booster doses were administered at 2-week intervals. Mice were challenged intravenously with 200 PFU of $ZIKV_{PRVABC59}$ 3 weeks after the final dose, and sera were collected on days 1, 2, and 3 post-challenge. **C** Anti-NS1 IgG endpoint titers measured by ELISA. Titers are expressed as the reciprocal of the serum dilution (log_{10} scale). The data represent mean responses ($n = 10$) ± SEM, and comparisons were performed using Mann–Whitney U tests. **D** Serum viral loads measured by RT-qPCR on days 1, 2, and 3 post-infection. Statistical comparisons between groups were performed on Log10 normalized data using One-way ANOVA with Tukey's multiple comparisons. *$P \le 0.05$, **$P \le 0.01$, ***$P \le 0.001$, ****$P \le 0.0001$.

cytotoxicity, and memory maintenance[35,61,70]. Our findings align closely with human immunogenicity data. El Sahly et al.[51] reported that NS3, NS5, and NS4B were dominant $CD8^+$ T cell targets in a cohort of U.S. patients, with NS4B recognized universally. Another study spanning six HLA class I alleles confirmed NS4B and NS5 as the most immunogenic proteins in diverse populations, mirroring the dominance of the NS4 epitopes in our model[50]. This concordance underscores the translational relevance of our approach and validates the BALB/c model as a physiologically relevant model for preclinical vaccine evaluation.

The immunodominance of NS3 and NS4B is conserved across flaviviruses. In YFV, TBEV, and WNV, NS3 and NS4 elicit strong $CD8^+$ responses[71–75], while live attenuated JEV vaccination with SA14-14-2 induces NS1- and NS3-specific T cells that cross-react with ZIKV[43]. DENV-specific T cells also cross-react with ZIKV[37], supporting the inclusion of these antigens in a pan-flavivirus vaccine. Building on our previous work with secreted NS1[44] we generated individual pNS3 and pNS4 constructs, then combined them into a single NS3/4 polyprotein vaccine for ease of manufacturing and administration. Both induced potent $CD8^+$ T cell

responses targeting replication-essential domains such as the NS3 protease and helicase, and NS4B, which is also an innate immune antagonist[27,76,77]. Thus, targeting of ZIKV NS3/4 should interrupt viral replication and restore host antiviral signaling.

ZIKV infection in BALB/c mice elicited robust, polyfunctional T cell responses against NS3 and NS4, providing a clear rationale for their inclusion as vaccine antigens. Consistent with prior studies demonstrating the protective efficacy of NS3-based vaccines, our NS3/4 polyprotein vaccine alone conferred significant viral control compared with unvaccinated animals, although not to the same extent as NS1. Importantly, when NS3/4 was combined with NS1, the cocktail produced a more consistent and rapid reduction in viraemia. This demonstrates that while NS3/4 responses are not individually superior to NS1, they add a measurable benefit in multivalent formulations by broadening the antiviral T cell repertoire. Similar patterns have been described in dengue, where NS3- and NS4B-specific T cells were among the most immunodominant responses, but their magnitude and polyfunctionality did not consistently correlate with protection at the individual level[78]. In this context, NS3/4 therefore provides additive breadth and robustness to the immune response, complementing rather than replacing NS1 as the dominant protective antigen.

A similar principle was observed in prior human studies, where not all T cell responses contributed equally to viral control. Kalimuddin et al.[79] reported that T cell responses targeting different orthoflaviviral proteins contributed unequally to control of RNAemia, with capsid-directed responses associated with control in that cohort. Importantly, the authors cautioned that this does not render NS3/NS5 responses redundant, as immunodominance may mask their contributions. Unlike capsid, which is poorly conserved across flaviviruses, NS1/NS3/NS4 are highly conserved and in our model, elicited high-avidity, polyfunctional responses, supporting the rationale for the combination of conserved NS antigens to enhance T cell breadth and subsequent viral control.

We used an immunocompetent BALB/c challenge model to evaluate both vaccine immunogenicity and protective efficacy. In our study, control animals consistently reached 10^6 ZIKV copies/mL within 24 h after challenge with 200 PFU ZIKV, confirming productive viral replication and providing a robust baseline for vaccine evaluation. This approach builds directly on the validated protocol described by Larocca et al.[56] and Pardi et al.[80], While adoptive transfer of T cells from immunocompetent to immunodeficient hosts may offer mechanistic insights, such models can introduce interpretative confounders and reduce physiological relevance.

Previous T cell-based vaccines demonstrated protection in mice using NS3-focused RNA[81] or DNA constructs[82] or epitope cocktails in combination with a subunit E protein vaccine[69,83]. Our approach extends this field by incorporating NS4B-specific immunity, identifying novel epitopes, and aligning mouse responses with human data. The polyprotein format also improves manufacturability and antigenic breadth, offering a more practical alternative to multi-epitope formulations.

Inclusion of NS1 alongside NS3/4 not only broadens T cell antigen coverage but also engages critical antibody-mediated effector functions. Anti-NS1 antibodies have been shown to mediate both antibody-dependent cell cytotoxicity and complement-dependent cytolysis, enhancing viral clearance through Fc-mediated pathways independent of neutralization[44,84]. These mechanisms can amplify antiviral efficacy, particularly in tissues or compartments less accessible to T cells.

Beyond mammalian hosts, NS1-specific antibodies may also reduce viral transmission by interfering with the vector. During ZIKV infection, secreted NS1 is taken up by *Aedes aegypti* mosquitoes during blood feeding, where it antagonizes innate immune responses by disrupting interferon-like signaling in the midgut, thereby enhancing viral replication and transmission potential[85,86]. Antibodies targeting NS1 can block this uptake and mitigate these immunosuppressive effects, reducing viral replication within the mosquito and potentially decreasing transmission efficiency[85–87]. Thus, anti-NS1 antibodies complement T cell-mediated antiviral responses by engaging both host and vector-directed mechanisms, reinforcing the value of its inclusion in a multi-antigen ZIKV vaccine strategy.

Our mapped epitopes overlap with immunodominant regions identified in human T cell studies, such as those reported by El Sahly et al.[51] and Eickhoff et al.[50], where NS3, NS4B, and NS5 emerged as the most consistently recognized targets across multiple HLA alleles. This suggests that the immunodominant responses observed in our BALB/c model are likely to be recapitulated in human populations. Furthermore, NS4B epitopes identified here contain conserved motifs across DENV, JEV, and YFV, indicating cross-reactive potential.

Attempts to engineer E-based vaccines[88–94] to minimize ADE have had only partial success, with residual enhancement observed due to FcγR-mediated mechanisms[89], escape mutations under antibody pressure[91,94] or persistent cross-reactive antibodies[93]. In contrast, NS proteins are not implicated in ADE and elicit durable, cross-reactive T cell responses[36,37,43,95]. Together with their high conservation across flaviviruses, these properties reinforce NS proteins as rational candidates for next-generation ZIKV vaccines, with the potential to support broader flavivirus protection pending further evaluation.

We also considered translational feasibility. DNA vaccines are known for efficient $CD8^+$ T cell priming and have entered clinical use (e.g., ZyCoV-D for COVID-19[96]) or are in advanced clinical testing (VGX-3100 for HPV-associated neoplasia[97]). Their intrinsic stability and scalable production make them attractive for deployment in resource-limited settings, such as regions where ZIKV and DENV co-circulate. Although mRNA vaccines are also effective, recent studies suggest that LNP-DNA may induce superior $CD8^+$ T cell responses at lower doses[98], reinforcing DNA's value for T cell-focused vaccines. Furthermore, the standalone expression of NS1 as a secreted antigen provides modularity, allowing flexible integration with adjuvants or alternative platforms such as viral vectors and mRNA. Our findings reinforce this potential by demonstrating potent $CD8^+$ T cell responses using conventional plasmid DNA, which could be further amplified through modern delivery technologies.

Together, our data support the development of a multi-antigen DNA vaccine targeting conserved NS proteins to elicit potent $CD8^+$ T cell responses. This strategy avoids ADE, aligns with human immunodominance patterns, and leverages scalable vaccine platforms suited for outbreak preparedness. While our study focused on ZIKV viremia, future work should address placental and neurological protection and heterologous flavivirus challenge. Overall, this approach offers a rational path toward safe, effective, and broadly protective flavivirus vaccines.

Methods

ZIKV infection

Female BALB/c mice (6–8 weeks old) were infected i.v. (via tail vein) with 200 PFU of $ZIKV_{PRVABC59}$ as described previously[44]. For T cell kinetics, mice received FTA target cells on days 7, 14, or 35 post-infection. In a separate experiment, splenocytes were harvested for cytokine analysis. For vaccine efficacy, mice were i.v. (tail vein) challenged with 200 PFU of $ZIKV_{PRVABC59}$ 3 weeks after the last dose, and serum was collected (via submandibular vein) on days 1, 2, 3, and 7-days post-infection for VL assessment.

Mice immunizations

BALB/c mice ($n = 7–10$/group) were immunized intradermally into the ear pinnae with 50 μg (single) or 100 μg (cocktail) DNA vaccine in sterile PBS, following a prime–boost–boost regimen at 2-week intervals. Vaccines were delivered under isoflurane (2–4%, 0.5 L/min flow rate) anesthesia (25 μL/ear) using 31 G insulin syringes. Mice were monitored for adverse effects, with blood collected (via submandibular vein) on days 14, 28, and 42 for serology.

Euthanasia

At experimental endpoints, mice were placed in an acrylic induction chamber supplied with medical-grade CO_2. Gas was introduced by gradual fill at 20% of chamber volume min^{-1} (3 L min^{-1}) until ≥1 min after cessation of respiration. Mice were not pre-sedated, as the approved gradual-fill rate

produces rapid unconsciousness with minimal distress. Death was confirmed by the complete absence of respiration for ≥1 min, fixed dilated pupils, loss of corneal and palpebral reflexes, and no response to a paw-pinch stimulus. Splenocytes were harvested for ELISpot and FTA assays.

Peptides Peptide arrays spanning full-length ZIKV non-structural proteins (PRVABC59 strain) were used for epitope mapping and T cell assays. A 114-peptide NS1 array (13–15mers, 12-aa overlap; BEI Resources, NR-50534, https://www.beiresources.org/Catalog/BEIPeptideArrays/NR-50534.aspx.) and a 164-peptide Envelope array (15mers, 12-aa overlap; NR-50553, https://www.beiresources.org/Catalog/BEIPeptideArrays/NR-50554.aspx.) were sourced from BEI. NS2A/B (51 peptides) and NS4A/B (57 peptides) peptide arrays were synthesized by RoyoBiotech Co., Ltd. (Shanghai, China). Individual peptides for these arrays were 12-, 16-, or 18-mers, each overlapping by 11 amino acids. NS3 (153 peptides) and NS5 (160 peptides) arrays (15mers, 11-aa overlap) were provided by Prof. David H. O'Connor (UW-Madison). Peptides were used at 5 μg/mL for ICS, 10 μg/mL for in vivo FTA, and 4 μg/mL for ELISPOT.

Fluorescent target array assay (FTA)

To track T cell responses post-ZIKV infection (days 7, 14, 35), donor splenocytes were labeled with five CTV concentrations (0, 0.053, 0.197, 0.73, or 2.7 mM), pulsed with peptide pools spanning NS1 (P1–P4), NS2 (P1–P2), NS3 (P1–P5), NS4 (P1–P2), NS5 (P1–P5), or Env (P1–P6). Following 4-h incubation at 37 °C, cells were washed and pooled into five groups, each labeled with a distinct CFSE concentration (2.7, 0.82, 0.23, 0.08, or 0.02 mM). All cells were then pooled and labeled with CPD (10 mM), generating 25 unique target clusters per mouse.

For epitope-level mapping, an expanded FTA, using four CPD, six CFSE, and 4 or 5 CTV concentrations, was used to generate 90–96 unique clusters pulsed with overlapping 13–18mer peptides spanning NS1, NS3, NS4, and Env. Avidity was assessed by creating 50 clusters using five CTV (0–2.7 mM) and five CFSE (0.02–2.9 mM) concentrations.

For vaccine-specific assays, splenocytes pulsed with NS3 (P1–P5) or NS4 (P1–P2) pools were labeled with combinations of CTV, CFSE, and CPD to yield 6 (pNS3) or 3 (pNS4) clusters, which were injected into vaccinated or control mice. Flow cytometry data were analyzed with FlowJo v10.10. CTL activity was calculated as % killing = [(mock–peptide target)/mock] × 100. T-helper responses were assessed by CD69 GMFI on $B220^+$ targets (peptide–nil control).

Intracellular cytokine staining (ICS)

RBC-depleted splenocytes (2×10^6 cells/well) were stimulated with ZIKV peptides (5 μg/mL) for 12 h, followed by 4 h incubation with Brefeldin A. Positive and negative controls included stimulation cocktail and unstimulated cells, respectively. Cells were surface-stained with anti-CD3, CD4, CD8, CD44, and CD62L, then fixed, permeabilized, and stained intracellularly for IFN-γ, TNF-α, and IL-2. Samples were acquired on a BD FACSymphony and analyzed with FlowJo v10.7.1.

DNA vaccines

Codon-optimized NS3 and NS4 transgenes from the Brazil-ZKV2015 isolate (GenBank: KU497555) were synthesized (GeneArt) and cloned into the pVAX1 vector under a CMV promoter using NEBuilder HiFi DNA Assembly. Inserts were amplified by high-fidelity PCR, gel-purified, and assembled into linearized pVAX1. Constructs were transformed into *Escherichia coli* DH5α, screened by colony PCR, and confirmed by Sanger sequencing. Antigen expression was validated by immunofluorescence, and endotoxin-free plasmid DNA was prepared using Qiagen GigaPrep kits for immunization.

Indirect immunofluorescence assay

HEK293T cells (2.5×10^4/well) were seeded in 96-well plates and cultured in DMEM with 10% FBS and 1% penicillin–streptomycin at 37 °C, 5% CO_2. After 24 h, cells were transfected with 200 ng of DNA plasmids (p-tpaNS1, pNS3, pNS4, pNS3/4, or pVAX) using Lipofectamine LTX (ThermoFisher). At 48 h post-transfection, cells were fixed with 4% paraformaldehyde (15 min, RT), permeabilized with ice-cold methanol (20 min, −20 °C), and blocked with 2.5% BSA for 2 h at 37 °C.

NS1 was detected using sera from p-tpaNS1–vaccinated mice. NS3 and NS4 were detected using commercial rabbit mAbs (GeneTex: anti-NS3 GTX133309 and anti-NS4 GTX133311). After overnight incubation at 4 °C, cells were stained with Alexa Fluor 488–conjugated goat anti-mouse (A-11001) or goat anti-rabbit (A-11008) IgG secondary antibodies (1:300, 2 h, 37 °C, dark). Fluorescence was visualized on a Zeiss LSM-700 confocal microscope and analysed with Zen software.

IFN-γ ELISPOT

Splenocytes from vaccinated BALB/c mice were red blood cell–depleted and stimulated with NS3 (P1–P5) or NS4 (P1–P2) peptide pools (4 μg/mL/peptide) for 36 h at 37 °C, 5% CO_2. Multiscreen-IP plates (Merck Millipore) were pre-coated overnight at 4 °C with anti-mouse IFN-γ capture antibody (Mabtech, clone AN18), washed, and blocked with RPMI + 10% FBS (1 h, RT). After stimulation, IFN-γ secretion was detected using biotinylated anti-IFN-γ (clone R4-6A2, Mabtech), followed by streptavidin–alkaline phosphatase (Sigma). Plates were developed with BCIP/NBT substrate, washed with distilled water, and air-dried. Spot-forming units (SFUs) were quantified using an AID ELISpot Reader and expressed as SFU per 10^6 splenocytes after background subtraction.

ZIKV NS1 ELISA

Nunc MaxiSorp 96-well plates were coated overnight at 4 °C with ZIKV NS1 protein (1 μg/mL; Sino Biological) in PBS. Plates were washed with PBST and blocked with StartingBlock (5 min, RT). Serially diluted mouse sera were incubated for 1 h at 37 °C, followed by HRP-conjugated goat anti-mouse IgG detection. OD was measured at 492 nm. Endpoint titers were defined as the highest serum dilution exceeding a cutoff set at 2 SD above the mean OD of control (pVAX or naïve) sera.

Reverse transcription polymerase chain reaction (RT-PCR)

VL in BALB/c mice was assessed as previously described[44]. Viral RNA was extracted from serum using the IndiSpin QIAcube HT Pathogen Kit (Indical) on a QIAcube HT (Qiagen) and reverse transcribed with LunaScript RT SuperMix (NEB). qPCR targeting the ZIKV cap gene was performed on a ViiA 7 system using TaqMan Fast Advanced Master Mix (Applied Biosystems). Log-diluted RNA standards from wild-type ZIKV BeH815744 were reverse transcribed and included with each RT-PCR assay. VL were calculated as virus particles per ml.

Statistical analyses

All data were analyzed and generated using GraphPad Prism version 9.0 (GraphPad Software, Inc.) and IBM SPSS Statistics software. ICS radar plots were generated using OriginPro 2024b (OriginLab). Results were expressed as mean ± SEM. Depending on the dataset, statistical significance was assessed using one- or two-way ANOVA with Tukey's or Dunnett's post-hoc tests, or Mann–Whitney U tests with Benjamini–Hochberg false discovery rate (FDR) correction applied to control for multiple testing.*$P < 0.05$, **$P < 0.01$, ***$P < 0.001$, and ****$P < 0.0001$ considered significant.

Ethics statement

All animal work complied with the Australian Code for the care and use of animals for scientific purposes and was approved by the University of Adelaide Animal Ethics Committee. Mice were bred under SPF conditions and housed in HEPA-filtered IVCs (Aero 80, Tecniplast) at The Queen Elizabeth Hospital (Adelaide) animal facility.

Materials availability

All data needed to evaluate the conclusions in the paper are present in the paper and/or the Supplementary Materials. Additional data related to this paper may be requested from the authors.

Data availability

All data supporting the findings of this study are available within the paper and its Supplementary Information.

Received: 23 June 2025; Accepted: 12 December 2025;
Published online: 17 January 2026

References

1. Vasilakis, N. & Weaver, S. C. Flavivirus transmission focusing on Zika. Curr. *Opin. Virol* **22**, 30–35 (2017).
2. World Health Organization. Countries with Zika virus transmission and presence of vectors. World Health Organization, Geneva https://cdn.who.int/media/docs/default-source/documents/emergencies/zika/countries-with-zika-and-vectors-table_21-may-2024.pdf (2024). (accessed 21 May 2024).
3. (WHO), W.H.O Countries with current or past Zika virus transmission and reported presence of competent vectors—as of 21 May 2024. World Health Organization: Geneva, Switzerland, (2024) .
4. Calvet, G. A. et al. Detection and persistence of Zika virus in body fluids and associated factors: a prospective cohort study. *Sci. Rep.* **13**, 21557 (2023).
5. Almeida, R. D. N. et al. The cellular impact of the ZIKA virus on male reproductive tract immunology and physiology. *Cells* **9**, 1006 (2020).
6. Kurscheidt, F. A. et al. Persistence and clinical relevance of Zika virus in the male genital tract. *Nat. Rev. Urol.* **16**, 211–230 (2019).
7. Christoff, R. R. et al. Congenital Zika virus infection impairs corpus callosum development. *Viruses* **15**, 2336 (2023).
8. Ba, F. et al. Zika virus-related birth defects and neurological complications: a systematic review and meta-analysis. *Rev. Med. Virol.* **35**, e70019 (2025).
9. de Carvalho, N. S. et al. Zika virus and pregnancy: an overview. *Am. J. Reprod. Immunol.* **77**, e12616 (2017).
10. Moore, C. A. et al. Characterizing the pattern of anomalies in congenital Zika syndrome for pediatric clinicians. *JAMA Pediatr* **171**, 288–295 (2017).
11. Cao-Lormeau, V. M. et al. Guillain-Barré Syndrome outbreak associated with Zika virus infection in French Polynesia: a case-control study. *Lancet* **387**, 1531–1539 (2016).
12. Shahrizaila, N., Lehmann, H. C. & Kuwabara, S. Guillain-Barré syndrome. *Lancet* **397**, 1214–1228 (2021).
13. Christian, K. M., Song, H. & Ming, G. L. Pathophysiology and mechanisms of Zika virus infection in the nervous system. *Annu. Rev. Neurosci.* **42**, 249–269 (2019).
14. Beattie, J. et al. Zika virus-associated Guillain-Barré syndrome in a returning US traveler. Infect. *Dis. Clin. Pr.* **26**, e80–e84 (2018).
15. Uncini, A., Shahrizaila, N. & Kuwabara, S. Zika virus infection and Guillain-Barré syndrome: a review focused on clinical and electrophysiological subtypes. *J. Neurol. Neurosurg. Psychiatry* **88**, 266–271 (2017).
16. Cachay, R. et al. Case Report: multiorgan involvement with congenital Zika syndrome. *Am. J. Trop. Med. Hyg.* **103**, 1656–1659 (2020).
17. França, G. V. et al. Congenital Zika virus syndrome in Brazil: a case series of the first 1501 livebirths with complete investigation. *Lancet* **388**, 891–897 (2016).
18. Tebas, P. et al. Safety and immunogenicity of an anti-Zika virus DNA vaccine. *N. Engl. J. Med* **385**, e35 (2021).
19. Peng, Z. Y. et al. A review on Zika vaccine development. *Pathog. Dis* **82**, ftad036 (2024).
20. Thomas, S. et al. Antibody-dependent enhancement (ADE) and the role of complement system in disease pathogenesis. *Mol. Immunol.* **152**, 172–182 (2022).
21. Rathore, A. P. S. et al. Maternal immunity and antibodies to dengue virus promote infection and Zika virus-induced microcephaly in fetuses. *Sci. Adv* **5**, eaav3208 (2019).
22. Fowler, A. M. et al. Maternally acquired Zika antibodies enhance dengue disease severity in mice. *Cell Host Microbe* **24**, 743–750.e5 (2018).
23. Bardina, S. V. et al. Enhancement of Zika virus pathogenesis by preexisting antiflavivirus immunity. *Science* **356**, 175–180 (2017).
24. Crooks, C. M. et al. Previous exposure to dengue virus is associated with increased Zika virus burden at the maternal-fetal interface in rhesus macaques. *PLoS Negl. Trop. Dis.* **15**, e0009641 (2021).
25. George, J. et al. Prior exposure to Zika virus significantly enhances peak Dengue-2 viremia in rhesus macaques. *Sci. Rep.* **7**, 10498 (2017).
26. Katzelnick, L. C. et al. Zika virus infection enhances future risk of severe dengue disease. *Science* **369**, 1123–1128 (2020).
27. Lin, D. L. et al. The ER membrane protein complex promotes biogenesis of dengue and Zika virus non-structural multi-pass transmembrane proteins to support infection. *Cell Rep* **27**, 1666–1674.e4 (2019).
28. Pattnaik, A., Sahoo, B. R. & Pattnaik, A. K. Current status of Zika virus vaccines: successes and challenges. *Vaccines* **8**, 266 (2020).
29. Poland, G. A., Ovsyannikova, I. G. & Kennedy, R. B. Zika vaccine development: current status. *Mayo Clin. Proc.* **94**, 2572–2586 (2019).
30. Shrestha, B. & Diamond, M. S. Role of CD8+ T cells in control of West Nile virus infection. *J. Virol.* **78**, 8312–8321 (2004).
31. Wen, J. et al. CD4(+) T cells cross-reactive with dengue and Zika viruses protect against Zika virus infection. *Cell Rep* **31**, 107566 (2020).
32. Hassert, M. et al. Identification of protective CD8 T cell responses in a mouse model of Zika virus infection. *Front. Immunol.* **10**, 1678 (2019).
33. Hassert, M. et al. CD4+T cells mediate protection against Zika associated severe disease in a mouse model of infection. *PLoS Pathog* **14**, e1007237 (2018).
34. Pereira Neto, T. A. et al. Multifunctional T cell response in convalescent patients two years after ZIKV. *infection. J. Leukoc. Biol.* **108**, 1265–1277 (2020).
35. Lum, F. M. et al. Longitudinal study of cellular and systemic cytokine signatures to define the dynamics of a balanced immune environment during disease manifestation in Zika virus-infected patients. *J. Infect. Dis.* **218**, 814–824 (2018).
36. Weiskopf, D. et al. Comprehensive analysis of dengue virus-specific responses supports an HLA-linked protective role for CD8+ T cells. *Proc. Natl. Acad. Sci. USA* **110**, E2046–E2053 (2013).
37. Wen, J. et al. Dengue virus-reactive CD8(+) T cells mediate cross-protection against subsequent Zika virus challenge. *Nat. Commun.* **8**, 1459 (2017).
38. Chu, H. et al. CD8+ T-cell responses in flavivirus-naive individuals following immunization with a live-attenuated tetravalent dengue vaccine candidate. *J. Infect. Dis.* **212**, 1618–1628 (2015).
39. Elong Ngono, A. & Shresta, S. Cross-reactive T Cell immunity to dengue and Zika viruses: new insights into vaccine development. *Front. Immunol.* **10**, 1316 (2019).
40. Herrera, B. B. et al. Sustained specific and cross-reactive T cell responses to Zika and dengue virus NS3 in West Africa. *J. Virol* **92**, e01992–17 (2018).
41. Wen, J. et al. Identification of Zika virus epitopes reveals immunodominant and protective roles for dengue virus cross-reactive CD8(+) T cells. *Nat. Microbiol.* **2**, 17036 (2017).
42. Wang, R. et al. Japanese encephalitis vaccine generates cross-reactive memory T cell responses to Zika virus in humans. *J. Trop. Med* **2022**, 8379286 (2022).
43. Tarbe, M. et al. Japanese encephalitis virus vaccination elicits cross-reactive HLA-Class I-restricted CD8 T cell response against Zika virus infection. *Front. Immunol.* **11**, 577546 (2020).
44. Grubor-Bauk, B. et al. NS1 DNA vaccination protects against Zika infection through T cell–mediated immunity in immunocompetent mice. *Sci. Adv* **5**, eaax2388 (2019).

45. Zeng, J. et al. Mpox multi-antigen mRNA vaccine candidates by a simplified manufacturing strategy afford efficient protection against lethal orthopoxvirus challenge. *Emerg. Microbes Infect.* **12**, 2204151 (2023).
46. Xiong, F. et al. An mRNA-based broad-spectrum vaccine candidate confers cross-protection against heterosubtypic influenza A viruses. *Emerg. Microbes Infect.* **12**, 2256422 (2023).
47. Gummow, J. et al. A multiantigenic DNA vaccine that induces broad hepatitis C virus-specific T-cell responses in mice. *J. Virol.* **89**, 7991–8002 (2015).
48. Wijesundara, D. K. et al. Induction of genotype cross-reactive, hepatitis C virus-specific, cell-mediated immunity in DNA-vaccinated mice. *J. Virol* **92**, e02133–17 (2018).
49. Weiskopf, D. et al. Insights into HLA-restricted T cell responses in a novel mouse model of dengue virus infection point toward new implications for vaccine design. *J. Immunol.* **187**, 4268 (2011).
50. Eickhoff, C. S. et al. Identification of immunodominant T cell epitopes induced by natural Zika virus infection. *Front. Immunol.* **14**, 1247876 (2023).
51. El Sahly, H. M. et al. Clinical, virologic, and immunologic characteristics of Zika virus infection in a cohort of US patients: prolonged RNA detection in whole blood. *Open Forum Infect. Dis* **6**, ofy352 (2019).
52. Muthumani, K. et al. In vivo protection against ZIKV infection and pathogenesis through passive antibody transfer and active immunisation with a prMEnv DNA vaccine. *NPJ Vaccines* **1**, 16021 (2016).
53. Li, A. et al. A Zika virus vaccine expressing premembrane-envelope-NS1 polyprotein. *Nat. Commun.* **9**, 3067 (2018).
54. Medina-Magües, L. G. et al. mRNA vaccine protects against Zika virus. *vaccines* **9**, 1464 (2021).
55. Essink, B. et al. The safety and immunogenicity of two Zika virus mRNA vaccine candidates in healthy flavivirus baseline seropositive and seronegative adults: the results of two randomised, placebo-controlled, dose-ranging, phase 1 clinical trials. *Lancet Infect. Dis.* **23**, 621–633 (2023).
56. Larocca, R. A. et al. Vaccine protection against Zika virus from Brazil. *Nature* **536**, 474–478 (2016).
57. Pardy, R. D. et al. Analysis of the T cell response to Zika virus and identification of a novel CD8+ T cell epitope in immunocompetent mice. *PLoS Pathog* **13**, e1006184 (2017).
58. Nazerai, L. et al. Effector CD8 T cell-dependent Zika virus control in the CNS: a matter of time and numbers. *Front. Immunol.* **11**, 2020 (1977).
59. Elong Ngono, A. et al. Mapping and role of the CD8(+) T cell response during primary Zika virus infection in mice. *Cell Host Microbe* **21**, 35–46 (2017).
60. Schouest, B. et al. Pre-existing T cell memory against Zika virus. *J. Virol* **95**, e00132–21 (2021).
61. Hassert, M., Brien, J. D. & Pinto, A. K. Mouse models of heterologous flavivirus immunity: a role for cross-reactive T cells. *Front. Immunol.* **10**, 1045 (2019).
62. Derby, M. et al. High-avidity CTL exploit two complementary mechanisms to provide better protection against viral infection than low-avidity CTL. *J. Immunol.* **166**, 1690–1697 (2001).
63. Brehm, M. A., Daniels, K. A. & Welsh, R. M. Rapid production of TNF-α following TCR engagement of naive CD8 T cells1. *J. Immunol* **175**, 5043–5049 (2005).
64. Seder, R. A., Darrah, P. A. & Roederer, M. T-cell quality in memory and protection: implications for vaccine design. *Nat. Rev. Immunol.* **8**, 247–258 (2008).
65. Shukla, R. et al. Dengue and Zika virus infections are enhanced by live attenuated dengue vaccine but not by recombinant DSV4 vaccine candidate in mouse models. *EBioMedicine* **60**, 102991 (2020).
66. Halstead, S. B. Which dengue vaccine approach is the most promising, and should we be concerned about enhanced disease after vaccination? There is only one true winner. *Cold Spring Harb. Perspect. Biol.* **10**, a030700 (2018).
67. Katzelnick, L. C., Bos, S. & Harris, E. Protective and enhancing interactions among dengue viruses 1-4 and Zika virus. *Curr. Opin. Virol* **43**, 59–70 (2020).
68. Zhang, H. et al. The CD8+ and CD4+ T cell immunogen atlas of Zika virus reveals E, NS1 and NS4 proteins as the vaccine targets. *Viruses* **14**, 2332 (2022).
69. Sun, J. et al. Development of a novel ZIKV vaccine comprised of immunodominant CD4+ and CD8+ T cell epitopes identified through comprehensive epitope mapping in Zika virus infected mice. *Vaccine* **39**, 5173–5186 (2021).
70. Shouse, A. N., LaPorte, K. M. & Malek, T. R. Interleukin-2 signaling in the regulation of T cell biology in autoimmunity and cancer. *Immunity* **57**, 414–428 (2024).
71. van der Most, R. G. et al. Yellow fever virus 17D envelope and NS3 proteins are major targets of the antiviral T cell response in mice. *Virology* **296**, 117–124 (2002).
72. James, E. Yellow fever vaccination elicits broad functional CD4+ T cell responses that recognize structural and nonstructural proteins. *J. Virol* **87**, 12794–12804 (2013). ddie et al.
73. Blom, K. et al. Specificity and dynamics of effector and memory CD8 T cell responses in human tick-borne encephalitis virus infection. *PLoS Pathog* **11**, e1004622 (2015).
74. Brien, J. D., Uhrlaub, J. L. & Nikolich-Zugich, J. Protective capacity and epitope specificity of CD8(+) T cells responding to lethal West Nile virus infection. *Eur. J. Immunol.* **37**, 1855–1863 (2007).
75. Kim, S. et al. A novel T-cell receptor mimic defines dendritic cells that present an immunodominant West Nile virus epitope in mice. *Eur. J. Immunol.* **44**, 1936–1946 (2014).
76. Brand, C., Bisaillon, M. & Geiss, B. J. Organization of the flavivirus RNA replicase complex. WIREs. *RNA* **8**, e1437 (2017).
77. Wu, Y. et al. Zika virus evades interferon-mediated antiviral response through the co-operation of multiple nonstructural proteins in vitro. *Cell Discov* **3**, 17006 (2017).
78. Weiskopf, D. et al. Human CD8+ T-cell responses against the 4 dengue virus serotypes are associated with distinct patterns of protein targets. *J. Infect. Dis.* **212**, 1743–1751 (2015).
79. Kalimuddin, S. et al. Vaccine-induced T cell responses control Orthoflavivirus challenge infection without neutralizing antibodies in humans. *Nat. Microbiol.* **10**, 374–387 (2025).
80. Pardi, N. et al. Zika virus protection by a single low-dose nucleoside-modified mRNA vaccination. *Nature* **543**, 248–251 (2017).
81. Elong Ngono, A. et al. CD8+T cells mediate protection against Zika virus induced by an NS3-based vaccine. *Sci. Adv* **6**, eabb2154 (2020).
82. Gambino, F. et al. A vaccine inducing solely cytotoxic T lymphocytes fully prevents Zika virus infection and fetal damage. *Cell Rep* **35**, 109107 (2021).
83. Roth, C. et al. Zika virus T-cell based 704/DNA vaccine promotes protection from Zika virus infection in the absence of neutralizing antibodies. *PLoS Negl. Trop. Dis.* **18**, e0012601 (2024).
84. Bailey, M. J. et al. Antibodies elicited by an NS1-based vaccine protect mice against Zika virus. *mBio* **10**, e02861–18 (2019).
85. Liu, Y. et al. Evolutionary enhancement of Zika virus infectivity in Aedes aegypti mosquitoes. *Nature* **545**, 482–486 (2017).
86. Liu, J. et al. Flavivirus NS1 protein in infected host sera enhances viral acquisition by mosquitoes. *Nat. Microbiol.* **1**, 16087 (2016).
87. Machmouchi, D. et al. The NS1 protein of contemporary West African Zika virus potentiates viral replication and reduces innate immune activation. *PLoS Negl. Trop. Dis.* **18**, e0012146 (2024).
88. Slon-Campos, J. L. et al. A protective Zika virus E-dimer-based subunit vaccine engineered to abrogate antibody-dependent enhancement of dengue infection. *Nat. Immunol.* **20**, 1291–1298 (2019).
89. Tharakaraman, K. et al. Rational engineering and characterization of an mAb that neutralizes Zika virus by targeting a mutationally

constrained quaternary epitope. *Cell Host Microbe* **23**, 618–627.e6 (2018).
90. Berneck, B. S. et al. A recombinant Zika virus envelope protein with mutations in the conserved fusion loop leads to reduced antibody cross-reactivity upon vaccination. *Vaccines* **8**, 603 (2020).
91. Bailey Mark et al. Human monoclonal antibodies potently neutralize Zika virus and select for escape mutations on the lateral ridge of the envelope protein. *J. Virol.* **93**, e00405–19 (2019).
92. Fernandez, E. et al. Human antibodies to the dengue virus E-dimer epitope have therapeutic activity against Zika virus infection. *Nat. Immunol.* **18**, 1261–1269 (2017).
93. Yang, C. et al. Characterization of two engineered dimeric Zika virus envelope proteins as immunogens for neutralizing antibody selection and vaccine design. *J. Biol. Chem* **294**, 10638–10648 (2019).
94. Sun, H. et al. A dual-approach strategy to optimize the safety and efficacy of anti-Zika virus monoclonal antibody therapeutics. *Viruses* **15**, 1156 (2023).
95. Grifoni, A. et al. Prior dengue virus exposure shapes T cell immunity to Zika virus in humans. *J. Virol* **91**, e01469–17 (2017).
96. Khobragade, A. et al. Efficacy, safety, and immunogenicity of the DNA SARS-CoV-2 vaccine (ZyCoV-D): the interim efficacy results of a phase 3, randomised, double-blind, placebo-controlled study in India. *Lancet* **399**, 1313–1321 (2022).
97. Trimble, C. L. et al. Safety, efficacy, and immunogenicity of VGX-3100, a therapeutic synthetic DNA vaccine targeting human papillomavirus 16 and 18 E6 and E7 proteins for cervical intraepithelial neoplasia 2/3: a randomised, double-blind, placebo-controlled phase 2b trial. *Lancet* **386**, 2078–2088 (2015).
98. Tursi, N. J. et al. Modulation of lipid nanoparticle-formulated plasmid DNA drives innate immune activation promoting adaptive immunity. *Cell Rep. Med.* **6**, 102035 (2025).

Acknowledgements

This work was supported by a Project Grant from The Hospital Research Foundation Group (THRFG), Australia, and in part by a THRFG Mid-Career Fellowship awarded to B.G.B. and an Early-Career Fellowship awarded to M.G.M. R.S. is supported by an Australian Government Research Training Program (RTP) Scholarship. Z.A.D. is supported by a University of Adelaide/THRFG Joint Scholarship.

Author contributions

Project conception and supervision: B.G.B. and M.G.M. Vaccine design: R.S. Experimental execution: R.S., Z.A.M., A.E.L.Y., D.M.W., and Z.A.D. Data analysis and interpretation: R.S., Z.A.M., M.G.M., and B.G.B. Reagent and technical support: N.S.E., M.R.B., D.H.B., and D.H.O. Manuscript writing—original draft: R.S. and Z.A.M. Manuscript review and editing: all authors. R.S. and Z.A.M. contributed equally and should be considered joint first authors.

Competing interests

B.G.B. is an inventor on a granted patent related to this work filed by The University of Adelaide (US-20240123051-A1). All other authors declare that they have no competing interests.

Additional information

Supplementary information The online version contains supplementary material available at https://doi.org/10.1038/s41541-025-01356-x.

Correspondence and requests for materials should be addressed to Branka Grubor-Bauk.